

# Thermal Shock Behaviour of Magnesia–Hercynite-Spinel Composite Refractories

**Tuba (Aksoy) Bahtlı\***

Necmettin Erbakan University, Faculty of Engineering and Architecture, Department of Metallurgical and Materials Engineering  
Konya, Turkey  
[taksoy@konya.edu.tr](mailto:taksoy@konya.edu.tr)

**Cemal Aksel**

Anadolu University, Faculty of Engineering, Department of Material Science and Engineering  
Eskisehir, Turkey  
[caksel@anadolu.edu.tr](mailto:caksel@anadolu.edu.tr)

**Abstract—** The effects of incorporations of spinel into MgO–hercynite (M–H) compositions to improve thermal shock behaviour were investigated.  $R$ ,  $R'''$ ,  $R''''$  parameters were calculated, and thermal shock tests were performed. The fracture surfaces of materials before and after thermal shock test were examined using SEM. Parameters improving thermal shock behaviour of M–H–S materials at 500 and 1000 °C are interlinking and arresting or deviation of microcracks when reaching the spinel and hercynite grains or pores, coexistence of intergranular and transgranular fractures leading to longer service life.

**Keywords—** MgO, hercynite,  $FeAl_2O_4$ , spinel,  $MgAl_2O_4$ , composite, refractories, thermal shock, Hasselman parameters

## I. INTRODUCTION

In recent years the production of MgO-spinel bricks and MgO-hercynite bricks as alternatives to MgO-chrome brick have become widespread [1]. Magnesia based refractories have been widely used in cement rotary kilns and steel ladles due to their high melting point, no toxicity and good resistance to basic slags and clinker phases. However, they have some disadvantages, such as high thermal conductivity, poor thermal shock resistance and infiltration resistance against chemical attack. In order to improve these properties, some metal oxides and compounds such as  $SiO_2$ ,  $CaO$ ,  $Al_2O_3$ ,  $MgAl_2O_4$ ,  $Cr_2O_3$ ,  $ZrO_2$ ,  $CaZrO_3$  and  $FeAl_2O_4$  have been used as doping agent. These oxides may react with MgO to form a second phase which improves the process of sintering [2-4].

Magnesium aluminate spinel ( $MgAl_2O_4$ ) is an important component of magnesia based refractories [5]. MgO based spinel bricks are used in the cooling zone and in the upper side of the sintering zone of cement rotary kilns [6, 7]. MgO–spinel refractories containing a small amount of spinel display high resistance against thermo-mechanical stresses formed at high temperatures and resultant thermal shocks [8].

The resistance to sudden transient temperature change, thermal shock, of refractory materials is a subject of considerable practical interest which has been explored in detail over many years [9].

Magnesia-hercynite bricks have better coatability than magnesia-spinel bricks. Also have better thermal shock resistance, good corrosion resistance as magnesia-spinel bricks [10].

In this study, the thermal shock resistance and therefore the service life MgO-hercynite composite refractories were intended to be improved by spinel addition. The relationships between the mechanisms causing improvements in the thermal shock parameters of composite refractories and strength and fracture surfaces of the materials before and after thermal shock test were examined. Related thermal shock parameters (Hasselman parameters) expressing the ability of a material to resist these thermal stresses were defined.

## II. MATERIAL AND METHOD

### A. Material Preparation

Recipes were prepared by incorporating 5, 10 and 20%  $MgAl_2O_4$  spinel (S) by weight into MgO (M) based compositions containing 5, 10 and 20 30%  $FeAl_2O_4$  hercynite (H) by weight. Those recipes were shaped as  $\sim 230 \times 115 \times 65$  mm<sup>3</sup> dimensions by applying  $\sim 127.5$  MPa (300 bar) press pressure. Then, sintered nearly at 1550 °C temperature. The materials were cut into 2.5 cm  $\times$  2.5 cm  $\times$  15 cm bar according to the standards for mechanical testing and thermal shock resistance test.

### B. Hasselman Parameters

Hasselman parameters, which determine the fracture resistance of materials due to thermal stress/shock and used in estimation of maximum thermal resistance were calculated by following formulas:

$$R = \frac{\sigma_f(1-\nu_c)}{E\alpha_c} \quad (1)$$

where  $\sigma$  is the strength,  $\alpha$  is the thermal expansion coefficient,  $\nu$  is the Poisson's ratio and  $E$  is the elastic modulus of materials the bar thickness. The thermal shock resistance factors ( $R$ ) expressing the ability of a material to resist these thermal stresses, are defined in terms of these mechanical and physical properties.

$$R''' = \frac{E}{\sigma_f^2} \cdot \frac{1}{(1-\nu_c)} \quad (2)$$

$$R'''' = \frac{E}{\sigma_f^2} \cdot \frac{\gamma_{wof}}{(1-\nu_c)} \quad (3)$$

where  $\gamma_{wof}$  is the work of fracture of materials. A second set of parameters ( $R'''$  and  $R''''$ ) is applicable to the case of severe thermal environments, where thermal stress fracture cannot be avoided and the major requirement is to minimize the extent of crack propagation [11].

### C. Mechanical Testing-Strength

The materials were cut into 2.5 cm × 2.5 cm × 15 cm bar according to the standards. The strength( $\sigma$ ) were determined before and after thermal shock test by the 3-point bending method in Instron 5581 [12, 13].

### D. Thermal Shock Test

Thermal-shock was carried out using a standard quench procedure. Bars were suspended using wire in a vertical tube furnace which was heated to 500 and 1000 °C temperatures. Thermal shock tests were performed by sudden cooling in water from 500 and 1000 8C to 25 8C room temperature. Bars were dried in an oven at 110 °C, and broken by 3-point bending test mentioned in C (Mechanical testing). In other words, strength values determined in connection with thermal shock temperatures.

### E. Microstructure Analysis

SEM (scanning electron microscope) studies carried out with Zeiss Evo 50 device, the fracture surfaces of the materials before and after thermal shock test were investigated.

## III. RESULTS AND DISCUSSION

### A. Thermal Shock Parameters (Hasselman Parameters)

When the results of  $R$  parameter values were analyzed in Figure 1, generally  $R$  parameter values of MgO-hercynite-spinel materials were higher than the MgO-hercynite materials. The highest  $R$  parameter value was achieved in M-10%H-20%S material.

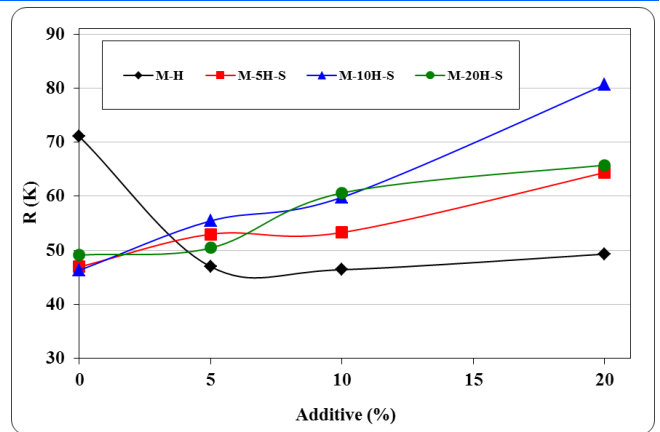


Fig. 1.  $R$  parameters of MgO-hercynite-spinel Composite Refractories.

$R'''$  parameter shows high resistance to the the crack propagation and the higher  $R'''$  values, the higher thermal shock resistance of material. MgO-hercynite composite materials had higher  $R'''$  thermal shock values than pure MgO (iron containing-MgO) material, and those values increased with increasing the amount of Hercynite addition.  $R'''$  value for the composite containing 20% Hercynite was approximately 10 times more than pure material (Figure 2).

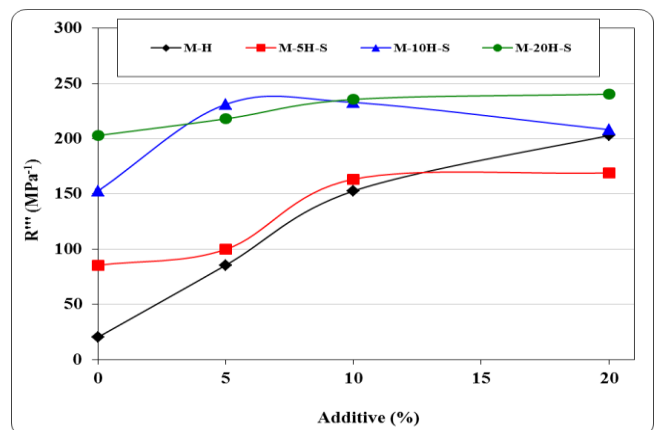


Fig. 2.  $R'''$  parameters of MgO-hercynite-spinel Composite Refractories.

Generally,  $R'''$  thermal shock parameter values of MgO-hercynite-spinel composite materials containing different ratios of spinel were higher than MgO-spinel materials. The highest  $R'''$  value was obtained M-20%H-20%S composite material (Figure 2).

$R''''$  parameter is used to estimate the resistance to the crack propagation of the material when subjected to thermal shock. MgO-hercynite composite materials had higher  $R''''$  thermal shock values than pure MgO material, and those values were significantly higher with increasing the amount of hercynite addition (Figure 3). For example, M-20%H composite materials showed 20 times higher resistance to crack propagation than pure MgO.

M-H-S materials had higher  $R''''$  thermal shock parameter values than MgO-Hercynite materials. The highest  $R''''$  value was reached in M-10%H-5%S

material, approximately 4.6 times enhancement was observed compared with M-5%H material.

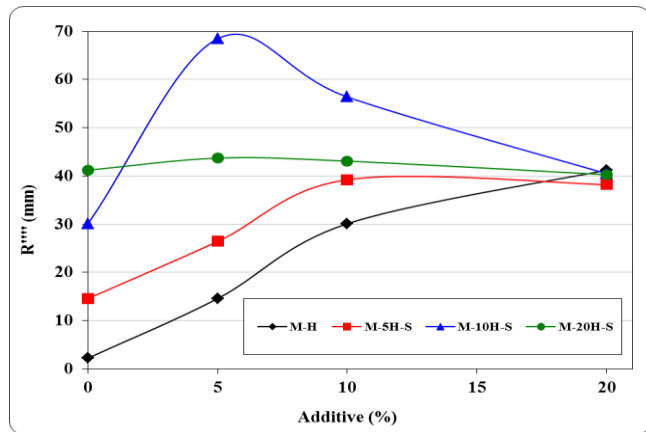


Fig. 3.  $R'''$  of MgO-hercynite-spinel Composite Refractories.

### B. Thermal Shock Test

The strength and the strength ratio values of the produced iron containing-MgO, MgO-hercynite and MgO-hercynite-spinel composite refractory materials were determined after the thermal shock test, according to different thermal shock temperatures (Figure 4, 5).

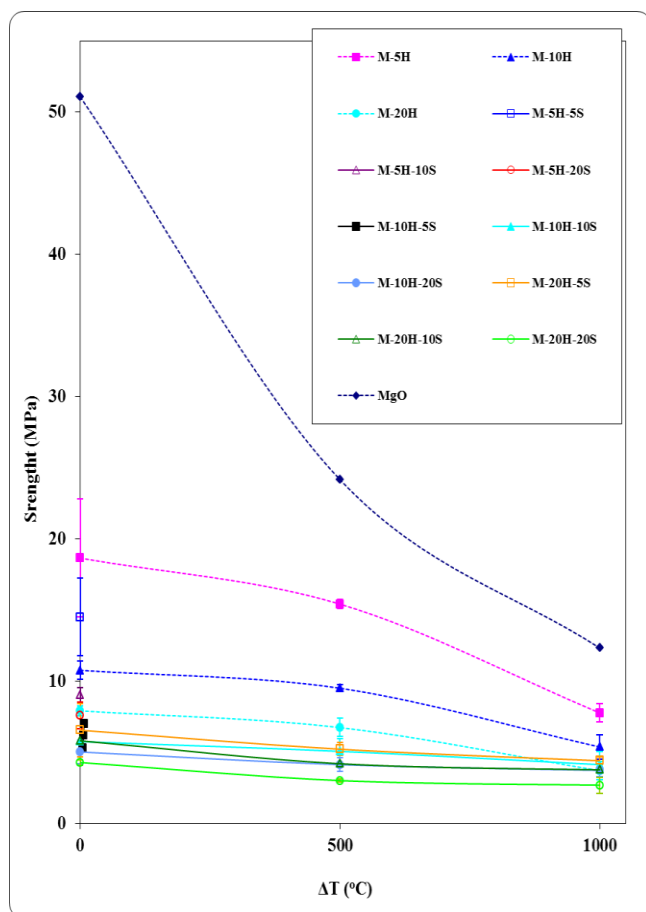


Fig. 4. Strength values of M-H and M-H-S composite refractories as a function of thermal shock temperatures.

In spite of the significantly reduction in the strength value of MgO (~ 4.1-fold) was observed, the reduction in the strength values of MgO-hercynite refractory materials were much less than MgO. During cooling from production temperatures, the large difference in the thermal expansion coefficient between MgO and hercynite ( $25-1000\text{ }^{\circ}\text{C}$ :  $\alpha_{\text{MgO}} = 13.6 \times 10^{-6}\text{ }^{\circ}\text{C}^{-1}$ ,  $\alpha_{\text{Hercynite}} = 9.0 \times 10^{-6}\text{ }^{\circ}\text{C}^{-1}$ ) generates large tensile stress around hercynite grains, resulted in interlinked microcracks that could stop the crack propagation occurred by thermal shock.

After thermal shock test at  $1000\text{ }^{\circ}\text{C}$ , M-5%H, M-10%H and M-20%H refractory materials had higher thermal shock resistance than pure MgO. Those sudden decrease in strength of MgO caused by the lack of spinel and hercynite reinforcements. This means that microcracks, occurred by mismatch of thermal expansion coefficients of MgO, hercynite and spinel ( $25-1000\text{ }^{\circ}\text{C}$ :  $\alpha_{\text{spinel}} = 7.6 \times 10^{-6}\text{ }^{\circ}\text{C}^{-1}$ ), couldn't been interlinked to each other. So, the length and the amount of big microcracks in MgO increased significantly.

Either at  $500\text{ }^{\circ}\text{C}$  or  $1000\text{ }^{\circ}\text{C}$ , the strength values of M-H-S materials generally had less or close to pure-MgO and MgO-hercynite materials. M-5%H-5%S had the highest strength at  $1000\text{ }^{\circ}\text{C}$  thermal shock test temperature among M-H-S materials. The mismatch of thermal expansion coefficients of MgO, hercynite and spinel caused interlinked microcracks. The big microcracks, occurred after thermal shock test, progressed in short distance in M-H-S materials, then the reduction in strength of those materials were limited.

After thermal shock test at  $500\text{ }^{\circ}\text{C}$ , although the strength ratio of iron containing-MgO was ~50%, the protected strength ratio values of MgO-hercynite composite materials were >80%.

After thermal shock test at  $1000\text{ }^{\circ}\text{C}$ , %, the protected strength ratio values of iron-containing MgO and MgO-hercynite composite materials were obtained as ~ 20% and >40% respectively. The highest protected strength ratio value was reached (~50%) in M-10%H refractory material among M-H materials.

As the protected strength ratio values of M-H-S composite materials were examined in Figure 5, either at  $500\text{ }^{\circ}\text{C}$  or  $1000\text{ }^{\circ}\text{C}$ , all materials had less strength loss, higher strength ratio than pure MgO and M-H materials. The highest protected strength ratio value was reached (79%) in M-5%H-5%S material among M-H-S materials.

In M-H and M-H-S materials whose initial strength values were lower, it wasn't observed big reduction in strength values unlike pure MgO. The reasons of those conditions were thought that the length and the amounts of microcracks occurred as a function of thermal shock test in M-H materials were smaller than MgO and those microcracks progressed in shorter distance.

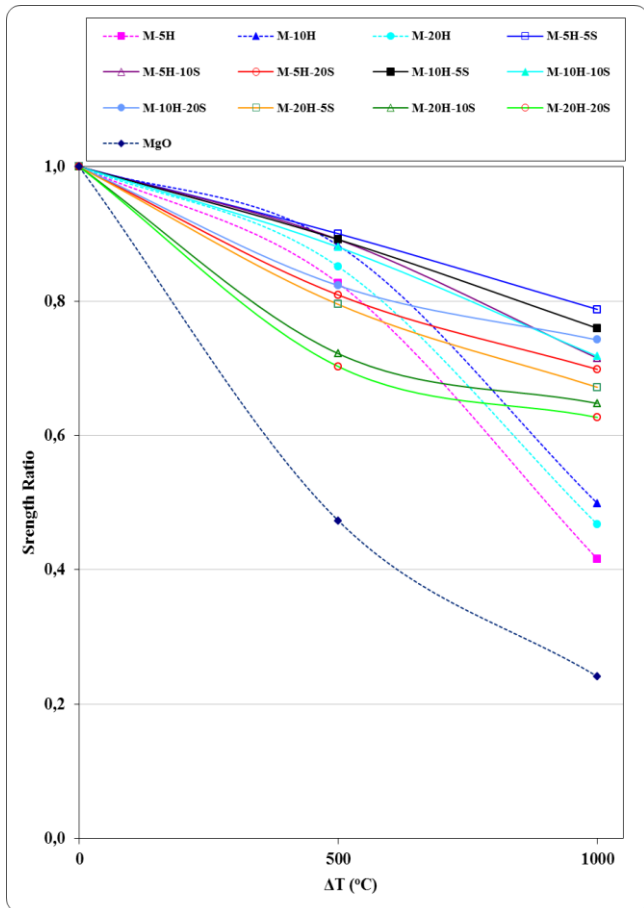


Fig. 5. Strength ratio values of M-H and M-H-S composite refractories as a function of thermal shock temperatures.

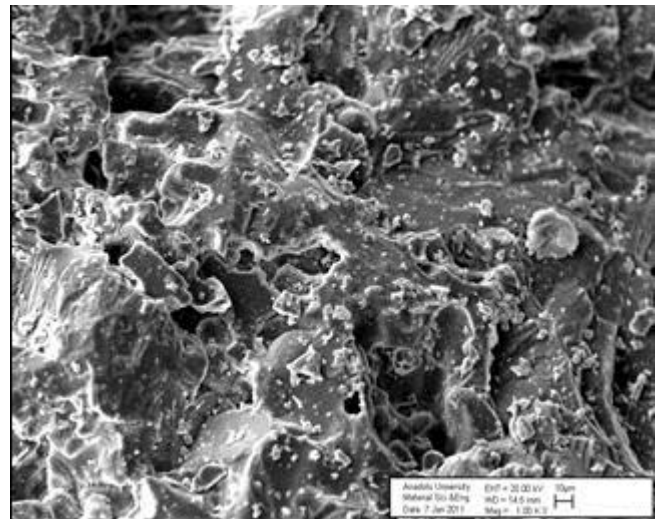
### C. Electron Microscope Characterization

The fracture surface images of iron containing-MgO refractory material before and after thermal shock test were given in Figure 6.

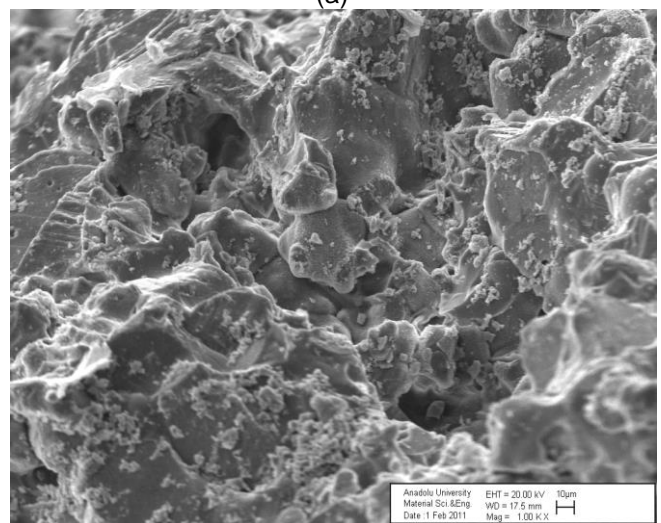
In general, before thermal shock tests, the pure iron-containing MgO material was exposed to transgranular cracks before thermal shock test. In particular, the cracks of medium-large-sized crystal grains were transgranular cracks type predominately. Due to this type of crack character, the material had relatively high resistance against the crack beginning, but the resistance to crack propagation was low (Figure 6-a).

After thermal shock test at 1000 °C, transgranular cracks type were predominately in iron containing-MgO (Figure 6-b). Because of its high thermal expansion coefficient, this material lost ~76% of its strength. The sudden decrease in strength of MgO caused transgranular type cracks in this material.

The fracture surface image of the refractory composite material formed by addition of 10% hercynite to iron-containing MgO before and after thermal shock test were given in Figure 7.



(a)

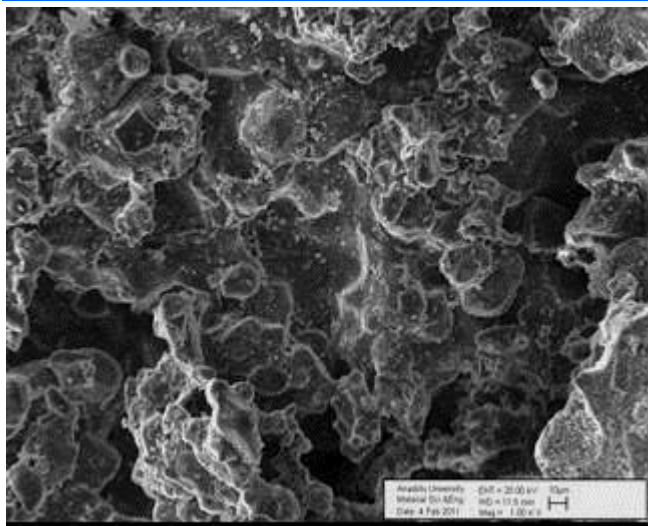


(b)

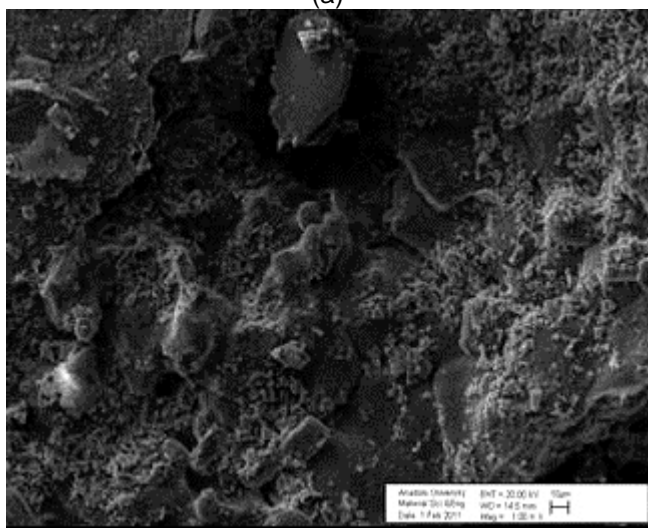
Fig. 6. The fracture surface image of iron-containing MgO material a) before thermal shock test, b) after thermal shock test at 1000 °C.

Large tensile stresses and microcracks were occurred in the structure due to thermal expansion coefficient differences between the MgO and hercynite grains during cooling after the sintering of composite materials. Microcracks in the material were connected to each other, stopped when they hercynite grains or changed their direction during the breaking of material. According to fracture surface image of MgO-hercynite material, either transgranular cracks or intergranular cracks were observed before thermal shock tests (Figure 7-a).

After thermal shock test at 1000 °C, in M-10%H material, either intergranular (more than transgranular) or transgranular cracks were observed (Figure 7-b). M-10%H material had smaller MgO grains than MgO material, then the big microcracks occurred after thermal shock tests progressed between those small MgO grains (intergranular cracks). intergranular cracks type caused higher thermal shock resistance of M-10 %H materials than pure-MgO.



(a)

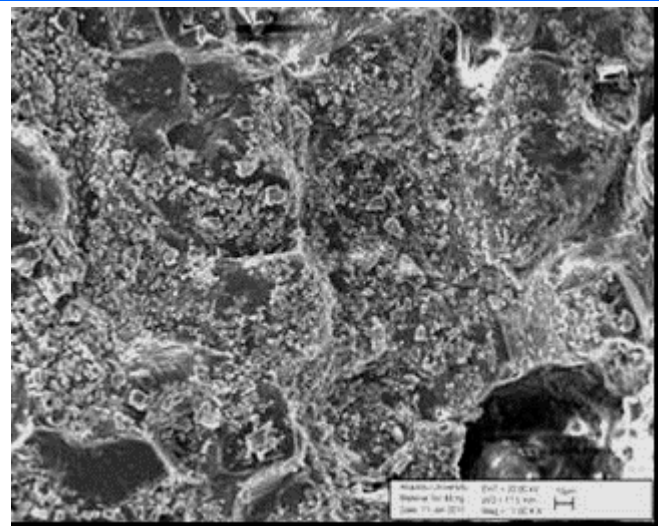


(b)

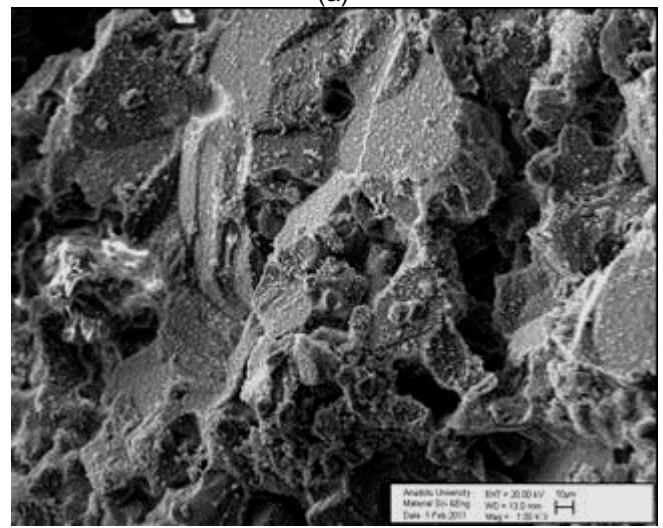
Fig. 7. The fracture surface image of M-10%H refractory material a) before thermal shock test, b) after thermal shock test at 1000 °C.

The fracture surface image of the M-5%H-5%S refractory composite material, that had the highest protected strength ratio value (79%), before and after thermal shock test were given in Figure 8.

Before thermal shock test, either intergranular or transgranular cracks were observed in M-5%H-5%S refractory material (Figure 8-a). After thermal shock test at 1000 °C, transgranular cracks type were predominant in M-5%H-5%S refractory material, but small amounts of intergranular cracks were, also (Figure 8-b). Those change in cracks type after thermal shock test was thought as an important parameter affected the protected strength ratio.



(a)



(b)

Fig. 8. The fracture surface image of M-5%H-5%S refractory material a) before thermal shock test, b) after thermal shock test at 1000 °C.

#### IV. CONCLUSIONS

Either at 500 °C or 1000 °C, the strength values of M-H-S materials generally had less or close to pure-MgO and MgO-hercynite materials. M-5%H-5%S had the highest strength at 1000 °C thermal shock test temperature among M-H-S materials.

Also, either at 500 °C or 1000 °C, all materials M-H-S had less strength loss, higher strength ratio than pure MgO and M-H materials. M-5%H-5%S material had the highest protected strength ratio value was reached (79%) in among M-H-S materials.

The mismatch of thermal expansion coefficients of MgO, hercynite and spinel (25–1000 °C:  $\alpha_{\text{MgO}} = 13.6 \times 10^{-6} \text{ } ^\circ\text{C}^{-1}$ ,  $\alpha_{\text{Hercynite}} = 9.0 \times 10^{-6} \text{ } ^\circ\text{C}^{-1}$ ,  $\alpha_{\text{spinel}} = 7.6 \times 10^{-6} \text{ } ^\circ\text{C}^{-1}$ ) caused interlinked microcracks that could avoid the propagation of big microcracks, occurred after thermal shock test, in M-H-S materials.

After thermal shock test at 1000 °C, transgranular cracks type were predominant in M-5%H-5%S

refractory material that was thought as an important parameter affected the protected strength ratio.

As the results were compared, it's observed that the thermal stress/shock parameters (Hasselman parameters) and results of thermal shock tests were compatible. In other words,  $R''''$  ve  $R''''''$  parameters indicating the resistance to propagation of crack, and R parameter expressing the ability of a material to resist these thermal stresses were indentified as reliable parameters could be used to determine the thermal shock resistance of MgO, M-H and M-H-S composite refractory materials.

#### ACKNOWLEDGMENT

This study was partly supported in part TUBITAK under project no: 106M394. We would like to express our gratitude to all employees and personnel of Konya Selcuklu Krom Magnezit Tugla A.S. for their support and the supplied equipments and raw materials.

#### REFERENCES

- [1] Pablo M. Botta, Estaban F. Aglietti, José M. Porto López, Mechanochemical synthesis of hercynite. *Materials Chemistry and Physics*, vol. 76, 104-109, 2002.
- [2] Peng C, Li N, Han B. Effect of zircon on sintering composition and microstructure of magnesia powder. *Sci Sinter* 2009;41:11–7.
- [3] Han B, Li Y, Guo C, Li N, Chen F. Sintering of MgO refractories with added WO<sub>3</sub>. *Ceram Int* 2007;33:1563–7.
- [4] Bartha P, Klischat HJ. Classification of magnesia bricks in rotary cement kilns according to

specification and service-ability. *ZKG Int* 1994;47:277–80.

[5] Pablo M. Botta, Estaban F. Aglietti, José M. Porto López, Mechanochemical synthesis of hercynite. *Materials Chemistry and Physics*, vol. 76, 104-109, 2002.

[6] Benbow J. Cement kiln refractories-down to basics. *Ind Miner*, 268, 37–45, 1990.

[7] Aksel C, Riley FL. Magnesia–spinel (MgAl<sub>2</sub>O<sub>4</sub>) refractory ceramic composites. In: Low IM, editor. *Ceramic matrix composites: microstructure, properties and applications*. USA: Woodhead Publishing Limited and CRC Press LLC; 359–99, 2006.

[8] Eusner GR, Hubble DH. Technology of spinel bonded periclase brick. *J Am Ceram Soc*, 43:292–6, 1960.

[9] Kingery, W. D., Factors affecting thermal stress resistance of ceramic materials, *J. Am. Ceram. Soc.*, 1955; 38(1): 3–15.

[10] Lui Huillin, 2008. Properties of magnesia-hercynite brick. *China's Refractories*, 17 [1], 26-28.

[11] Hasselman, D.P.H., "Thermal stress resistance parameters for brittle refractory ceramics: a compendium", *Am. Ceram. Soc. Bull.*, **49** [12], 1033-1037, 1970.

[12] Standard Test Methods for flexural strength of advanced ceramics at ambient temperature. In *Annual Book of ASTM Standards*, Designation: C1161-90, 15.01, 327–333, 1991.

[13] Standard Test Methods for flexural properties of unreinforced and reinforced plastics and electrical insulating materials. In *Annual Book of ASTM Standards*, Designation: D790M-86, 08.01, 290–298, 1988.